Hybrid adaptive block truncation coding for image compression

Ching-Yung Yang
Ja-Chen Lin
National Chiao Tung University
Institute of Computer and Information Science
Hsinchu, Taiwan 300
E-mail: jclin@cis.nctu.edu.tw

Abstract. A hybrid adaptive block truncation coding (HABTC) method is presented to improve block truncation coding (BTC)-related compression methods for gray-level images. The basic idea behind the method is to use various coding schemes to take advantage of local image characteristics. A simple linear interpolation coding scheme and a very basic predictive coding scheme are used to improve the compression ratio of the homogeneous area of the image. Moreover, a four-level BTC, whose thresholds are obtained using a radius-weighted mean (RWM), is applied to encode the inhomogeneous area. The bits per pixel/peak SNR (bpp/PSNR) values listed in many other BTC-related papers are cited and compared with ours. It is found that reasonable compression ratio is obtained by the proposed HABTC method and the visual quality of the decoded images is also acceptable. [S0091-3286(97)00104-9]

Subject terms: image compression; hybrid adaptive block truncation coding; linear interpolation coding; predictive coding; radius weighted mean; vector quantization.

Paper 05036 received Mar. 2, 1996; revised manuscript received Sep. 11, 1996; accepted for publication Sep. 12, 1996.

1 Introduction

Block truncation coding (BTC) is a simple lossy compression technique for digitized images. The main drawback of the conventional BTC algorithm is its relatively high bit rate (for example, 2 bits/pixel if each block is of size 4×4). Although the compression ratio of the BTC algorithm is inferior to other block-based encoding methods, such as the transform coding[1] and vector quantization[2] (VQ) techniques, BTC gained popularity due to its practical usefulness. Since the BTC algorithm was first introduced by Delp and Mitchell[3] in 1979, it has been modified in various ways. Based on the preservation of the first sample moment and the first absolute central moment, Lema and Mitchell[4] proposed the absolute moment BTC (AMBTC) algorithm to lower the bits per pixel (bpp) required by BTC. Udpikar and Raina[5] also developed a fast implementation approach to BTC with performance similar to that of the AMBTC. To reduce the bit rate further, Udpikar and Raina[6] applied the VQ technique to quantize the BTC encoding results; either the bitmap vectors or the gray-level vectors (or both) are quantized. When both are quantized, the bpp is 1.0 if both codebooks have size 256. Efrati et al.[7] presented the BTC-classification VQ (BTC-CVQ) technique that combines the classification technique of vector quantization with the BTC algorithm. The visual quality of the decoded image was substantially improved, but the coding efficiency was restricted to a moderate bit rate (usually 1.50 bpp). Wu and Coll[8] quantized the BTC coding results by applying VQ to the bitmap, and the discrete cosine transform (DCT) to the high- and low-mean subimages. Their BTC-VQ-DCT, when applied to the image ''Lena,'' had a peak SNR (PSNR) value 30.56 at 0.6875 bpp.

From the preceding review, we can see that the resulting bit rate produced by these modified versions of the BTC algorithms are still not good. In this paper, we therefore try to improve the bit rate of the BTC algorithm by combining some other techniques with BTC. To achieve this goal, we take advantage of the well-known fact that most natural images can be segmented into regions of widely varying perceptual importance.[7] A linear interpolation coding scheme and a predictive coding scheme are applied to encode the homogeneous blocks of which the gray values vary constantly. As for the inhomogeneous blocks, we quantize the gray values in each block into four levels by using a four-level radius-weighted mean (RWM) BTC modified from the conventional two-level BTC.

This paper is organized as follows. In Sec. 2, we describe the proposed hybrid adaptive block truncation coding (HABTC) for image compression. An optional version HABTC-VQ, which enhances HABTC with VQ, is also provided in Sec. 2.2.2. Simulation results are presented in Sec. 3. The compression performance of the proposed HABTC method is compared there with those of the other BTC-related methods, including the AMBTC, BTC-CVQ, VQ-interpolative BTC (VQ-IBTC) (Ref. 9), VQ-BTC (Ref. 10), hybrid VQ (HVQ) (Ref. 11), BTC-VQ-DCT, etc. Section 4 concludes the paper.

2 Proposed HABTC Method

Let an input image be partitioned into nonoverlapping blocks of size 4×4. Each block is first classified into a homogeneous block or an inhomogeneous block according to the statistical characteristics of that block. More precisely, a block is judged to be homogeneous if and only if

the standard deviation σ of the gray values of the block is less than a threshold value T_σ. Blocks that are not homogeneous will be referred to as inhomogeneous blocks. To code effectively, the homogeneous blocks are classified further into three categories, namely, interpolatable blocks, predictive blocks, and uniform blocks. Homogeneous blocks are transmitted using quite few bits. As for inhomogeneous blocks, they are quantized using a four-level BTC. To transmit the 32-bit allocation map generated by this four-level BTC, there are two versions: without VQ or with VQ. Usually, the version without VQ is suggested, unless a bpp lower than 0.57 is expected. Note that without VQ means that the original 32-bit map is transmitted directly. As for the version with VQ, we divide the inhomogeneous blocks into edge blocks and texture blocks depending on whether or not they contain edges. Then, a texture codebook is used to imitate the maps of texture blocks, and four edge codebooks (horizontal, vertical, diagonal, and antidiagonal, respectively) are used to imitate the maps of edge blocks. Traditionally, whether a block contains edges or not can be known by applying a standard edge detection operator such as the Sobel or Prewitt operator. In this paper, however, we use a faster and simpler approach suggested by Dondes and Rosenfeld[12] by measuring the minimum total variation (MTV) of the block. Note that the MTV measure is also capable of detecting the four kinds of the orientations (that is, horizontal, vertical, diagonal, and antidiagonal) of the edge existing in the edge blocks. To improve clarity, the scheme of the proposed HABTC is described in Fig. 1. The details are explained in the next two subsections.

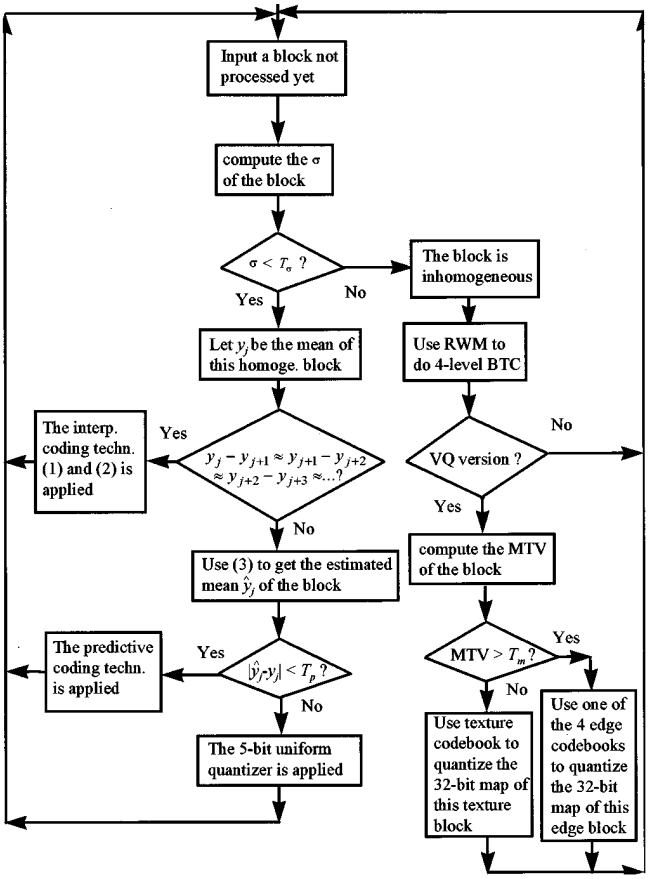

Fig. 1 Scheme of the proposed HABTC method.

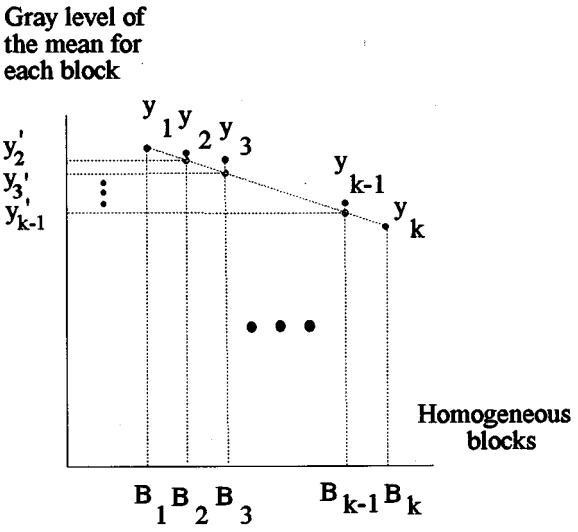

Fig. 2 Decoding of the homogeneous blocks $\{B_2, B_3, \ldots, B_{k-1}\}$ using the means y_1 and y_k of blocks B_1 and B_k [see Eqs. (1) and (2)].

2.1 *Homogeneous Block Coding*

Since most of the improved versions of the BTC algorithms are still inefficient for coding homogeneous blocks, we try to use as few bits as possible to represent these blocks. To achieve this goal, three effective techniques called linear interpolation coding, predictive coding, and uniform coding are employed in our method to encode the homogeneous blocks. To increase the compression efficiency without degrading the visual quality too much in the encoding of a homogeneous block, the sequence of the linear interpolation coding test, predictive coding test, and uniform coding process appearing in Fig. 1 are best not changed. (We had tried to switch the sequence of the linear interpolation coding test with the predictive test, and it was found that although the compression ratio increased a little, the PSNR of the reconstructed images degraded somewhat too much.)

2.1.1 *Part I: the bunch of interpolatable blocks*

For each scan line of the blocks (that is, the blocks located in the same row), if there are a series of homogeneous blocks connected together and if the difference between the means of each two adjacent blocks is almost constant (the variation of the differences is below a certain threshold T_i), then we can use an interpolation technique to quantize the blocks. The interpolation policy is illustrated in Fig. 2. Without loss of generality, let $B_1, B_2, \ldots, B_k$ denote a series of homogeneous blocks that are adjacent to one another, and let their corresponding means be $y_1, y_2, \ldots, y_k$, respectively. If $y_2 - y_1 \approx y_3 - y_2 \approx y_4 - y_3 \approx \cdots \approx y_k - y_{k-1}$, that is, if the means change at a rate that is almost constant, then we may estimate the values y_p by

$$y_p \approx y'_p = y_1 + (p-1) \times s \quad \forall 2 \leq p \leq k-1, \tag{1}$$

where s is a slope defined by

$$s=\frac{y_k-y_1}{k-1}. \tag{2}$$

Since there are three kinds of homogeneous blocks to be encoded in our HABTC method, we use three category indices {10;11;01} to distinguish them (the category index 00 is reserved for inhomogeneous blocks). The kind of block discussed in this paragraph uses 10 as its category index. In other words, for the k blocks $B_1,B_2,\ldots,B_k$, we transmit only the sequence $\{(10),y_1,k-2,y_k\}$, where 10 stands for category classification, and $k-2$ denotes the number of ''intermediate'' blocks $\{B_2,B_3,\ldots,B_{k-1}\}$ whose means are not transmitted and thus will require the help of Eqs. (1) and (2) to recover. The receiver then uses Eqs. (1) and (2) to obtain $\{y_1,y_2',y_3',\ldots,y_{k-1}',y_k\}$ before using these (exact or approximated) means to reconstruct homogeneous blocks B_1 through B_k. In this example, the bunch of the k blocks $B_1,B_2,\ldots,B_k$ are referred to as the interpolatable blocks, because we do not transmit means y_2 to y_{k-1}, but instead, we interpolate y_1 and y_k to obtain the estimated values y_2' to y_{k-1}' for the intermediate blocks. The number of bits required to encode the whole bunch of the k blocks $\{B_1,B_2,\ldots,B_k\}$ is only 21. That is, 2 bits for the category classification, 16 bits for the mean value of blocks B_1 and B_k at the two ends, and 3 bits to record $k-2$, i.e., to record the length of the intermediate blocks. [We have assumed that $1\leqslant k-2\leqslant 8=2^3$, i.e., $3\leqslant k\leqslant 10$, because a large value of k (more than 10) is seldom encountered in the real applications.]

2.1.2 *Part II: predictive blocks*

For the predictive blocks, nothing but the category classification bits are transmitted. The reconstructed mean $\hat{y}_{i,j}$ of the block is obtained by a commonly seen formula:

$$\hat{y}_{i,j}=0.75\hat{y}_{i,j-1}-0.5\hat{y}_{i-1,j-1}+0.75\hat{y}_{i-1,j}, \tag{3}$$

where $\hat{y}_{i,j-1}$, $\hat{y}_{i-1,j-1}$, and $\hat{y}_{i-1,j}$, are the reconstructed means (can either be lossless or lossy) of the left neighbor, upper-left neighbor, and upper neighbor of the block (i,j), respectively. In other words, the mean of the predictive blocks can not be reconstructed without the help of its three neighboring blocks. Consequently, there are only 2 bits (because the category index of the predictive block is 11) required to encode a predictive block. To avoid the severe degradation, the estimated mean $\hat{y}_{i,j}$ of the block is tested against the true mean $y_{i,j}$ each time to determine whether the predictive coding approach should be applied or not.

2.1.3 *Part III: uniform blocks*

Finally, a homogeneous block that cannot be encoded by either the interpolation coding or predicting coding technique is referred to as the smooth block. Since the gray values do not vary much inside the blocks, it is intuitive that the block can be represented by its mean. Instead of using 8 bits to encode the smooth block, we use 5 bits (uniform quantizer) to quantize the mean of the block so as to reduce the bit rate. The coding format of the smooth block is $\{(01),y_q\}$, where 01 indicates the ''smooth'' category of the block. The number of bits used to encode a smooth block is therefore 7. Note that only 5 bits are used to generate the 32-level uniform quantization needed here, although in Sec. 2.1.1 either y_1 or y_k did use the finer 256-gray-level system because the precision of the y_1 and y_k values will affect further the gray values of some other blocks B_2 to B_{k-1}.

2.2 *Inhomogeneous Block Coding*

2.2.1 *Four-level BTC using RWM*

The $4\times4=16$ gray values g_1 to g_{16} of an inhomogeneous block are quantized to four levels $\overline{x_{ll}}$, $\overline{x_{lh}}$, $\overline{x_{hl}}$, and $\overline{x_{hh}}$ according to the following procedure. First, we use the RWM (Ref. 13) of $G=\{g_1\ldots g_{16}\}$ as the bisection threshold to split G into two subsets L and H. Then the RWM of L is used to split L into two smaller subsets LL and LH. Similarly, the RWM of H is used to split H into two smaller subsets HL and HH. Now, the average of the gray values falling in LL is computed and called as $\overline{x_{ll}}$. Analogous statements hold for $\overline{x_{lh}}$, $\overline{x_{hl}}$, and $\overline{x_{hh}}$. Since the 4×4 block is quantized to four levels, each pixel i will need 2 bits to indicate which of the four levels is used to replace the gray values g_i. Therefore, an allocation map of $2\times(4\times4)=32$ bits is needed to indicate the spatial allocation of the four levels. As for the four representation gray values $\{\overline{x_{ll}},\overline{x_{lh}},\overline{x_{hl}},\overline{x_{hh}}\}$ themselves, to increase the compression ratio, instead of transmitting these four values directly, we transmit the $\{\alpha,\delta,\delta_h,\delta_l\}$ defined by

$$\alpha=(\overline{x_{hh}}+\overline{x_{hl}})/4+(\overline{x_{lh}}+\overline{x_{ll}})/4, \tag{4}$$

$$\delta=(\overline{x_{hh}}+\overline{x_{hl}})/4-(\overline{x_{lh}}+\overline{x_{ll}})/4, \tag{5}$$

$$\delta_h=(\overline{x_{hh}}-\overline{x_{hl}})/2, \tag{6}$$

and

$$\delta_l=(\overline{x_{lh}}-\overline{x_{ll}})/2. \tag{7}$$

With the definition of α, δ, δ_h, and δ_l just given, it is easy to prove that $\alpha+\delta\pm\delta_h$ gives us $\overline{x_{hh}}$ and $\overline{x_{hl}}$, while $\alpha-\delta\pm\delta_l$ gives us $\overline{x_{lh}}$ and $\overline{x_{ll}}$. In this paper, we quantize α, δ, δ_h, and δ_l to, respectively, 6, 5, 4, and 4 bits. Therefore, an inhomogeneous block is transmitted as $\{(00);\alpha,\delta,\delta_h,\delta_l;$ 32-bit allocation map$\}$ using $2+(6+5+4+4)+2(4\times4)=53$ bits. Here, 00 is the category index for inhomogeneous blocks.

In the preceding paragraph, the reason that RWM was used was because RWM can bisect a data set into two classes more efficiently than many other kinds of bisection methods do. To show this, we performed an extra experiment. Suppose that each of the $512/4\times512/4$ blocks is to be quantized into two levels. (In other words, temporarily assume that two-level BTC is to be used throughout the whole image.) Then, it can be seen from the middle column of Table 1 that obtaining optimal[14] bisection threshold for each block is time-consuming. However, from the rightmost column of Table 1, we can see that using RWM as the bisection threshold can give a nearly optimal PSNR within a short processing time.

2.2.2 *HABTC-VQ (the optional version with VQ)*

If we want to increase the compression ratio further, then the 32-bit allocation map of each inhomogeneous block can

Table 1 The PSNR and CPU time (in seconds) for several two-level BTC algorithms.

Images \ Bisect. Point	Conventional Mean[5] (PSNR/time)	Optimal Mean[14] (PSNR/time)	Iterated Mean[7] † (PSNR/time)	RWM (PSNR/time)
"Lena"	33.85/0.45	34.45/4.63	34.20/1.18	34.39/0.93
"Jet"	32.65/0.45	33.41/4.40	33.19/1.18	33.36/0.93
"Peppers"	34.06/0.45	34.71/4.66	34.47/1.18	34.65/0.93

†For each block, the two-level BTC algorithm[7] is applied three times, but the bisection point changed from iteration to iteration. The bisection point at the $(i+1)$'th iteration is $(\bar{y}_{high}+\bar{y}_{low})/2$, where $\bar{y}_{low}$ and $\bar{y}_{high}$ represent the low and high means of the block, respectively, of the i'th iteration.

be quantized using fewer bits by the VQ technique. But this quantization is not suitable if high PSNR (such as 38 dB for ''Lena'') is desired. In fact, our experience told us that, if the compression ratio is lower than 14 (or equivalently, if bpp is higher than 0.57), then using the version with VQ is not worthy, because the PSNR is degraded too much by VQ for compression ratio falling in the low range.

The version with VQ, called as HABTC-VQ, is introduced here. Note that, to reduce the time needed to find the nearest code word from the codebook, we do not suggest the use of a single codebook for all inhomogeneous blocks. Instead, the inhomogeneous blocks are classified further as edge blocks and texture blocks. Each of these two categories has its own codebook. The detail are as follows.

Part I: texture blocks. An inhomogeneous block contains no edge is classified as a texture block. (In Part II, we introduce how to use MTV to distinguish edge blocks from texture blocks.) In HABTC-VQ, a texture codebook of size $2^{10}=1024$ is used to reproduce approximately the 32-bit allocation map for each texture block. Therefore, the encoding sequence for a texture block is $\{(000);\alpha,\delta,\delta_h,\delta_l;I_t\}$. Here, 000 denotes that the inhomogeneous block is in fact a texture block, $(\alpha,\delta,\delta_h,\delta_l)$ are as stated in Sec. 2.2.1, and I_t is the index used to obtain the texture-map pattern selected from the texture codebook. The number of bits required to encode a texture block is $3+(6+5+4+4)+10=32$.

Part II: edge blocks. An inhomogeneous block is classified as an edge block if only if the MTV of the block is greater than a predetermined threshold value T_m. (An inhomogeneous block that is not an edge block is then called a texture block.) Without loss of generality, let the 4×4 gray values of an inhomogeneous block be as shown in Fig. 3. The measure of the MTV is defined by

$$\mathrm{MTV}=|\mathrm{HTV}-m|+|\mathrm{VTV}-m|+|\mathrm{DTV}-m|+|\mathrm{ADTV}-m|, \tag{8}$$

where $m=(\mathrm{HTV}+\mathrm{VTV}+\mathrm{DTV}+\mathrm{ADTV})/4$. Here, HTV, VTV, DTV, and ADTV denote the variations along the horizontal, vertical, diagonal, and antidiagonal directions, respectively. They are defined as follows (see Fig. 3):

$$\mathrm{HTV}=(|a-b+|b-c|+|c-d|+|e-f|+|f-g|+|g-h|+|i-j|+|j-k|+|k-l|+|m-n|+|n-o|+|o-p|)/12, \tag{9}$$

$$\mathrm{VTV}=(|a-e|+|e-i|+|i-m|+|b-f|+|f-j|+|j-n|+|c-g|+|g-k|+|k-o|+|d-h|+|h-l|+|l-p|)/12, \tag{10}$$

$$\mathrm{DTV}=(|b-e|+|c-f|+|f-i|+|d-g|+|g-j|+|j-m|+|h-k|+|k-n|+|l-o|)/9, \tag{11}$$

and

$$\mathrm{ADTV}=(|c-h|+|b-g|+|g-l|+|a-f|+|f-k|+|k-p|+|e-j|+|j-o|+|i-n|)/9. \tag{12}$$

Experimental evidence[12] indicates that the technique for measuring the MTV can detect not only the existence of the edges, but also the orientations of the edges. According to the orientation of edges, we have four kinds of edge-codebooks, namely, horizontal, vertical, diagonal, and antidiagonal. Each of these four codebooks has size $2^9=512$, and each code word is a typical 32-bit allocation map for some edge blocks. Therefore, the coding sequence of the edge blocks is $\{(001);\alpha,\delta,\delta_h,\delta_l;C_e,I_e\}$. Here, 001 denotes that the inhomogeneous block is in fact an edge block; $(\alpha,\delta,\delta_h,\delta_l)$ are as stated in Sec. 2.2.1; C_e is a 2-bit index used to distinguish the four possible edge-codebooks; and I_e is a 9-bit index used to indicate the 512 possible code words kept in the edge-codebook identified by C_e. The number of bits required to encode an edge blocks is therefore $3+(6+5+4+4)+2+9=33$ bits.

a	b	c	d
e	f	g	h
i	j	k	l
m	n	o	p

Fig. 3 Inhomogeneous block with 16-pixel gray values [see Eqs. (9) to (12)].

Fig. 4 Three original images: (a) ''Lena,'' (b) ''Jet,'' and (c) ''Peppers.''

3 Experimental Results

The proposed HABTC method was implemented on a Sun SPARC 10 workstation. Three 512×512 gray-scale images with 8 bpp, as shown in Fig. 4, namely, ''Lena,'' ''Jet,'' and ''Peppers,'' were tested. Many researchers used the PSNR as a measuring tool to gauge the image quality. The PSNR is defined as

$$\mathrm{PSNR}=10\times\log_{10}\frac{255^2}{\mathrm{MSE}}\ (\mathrm{dB}), \tag{13}$$

where the MSE is the mean square error. Although the PSNR does not correlate quite well with the perceived image quality, it does provide some information of the relative performance. We therefore use it in this section. A simple smoothing procedure was applied to the decoded images to alleviate somewhat the blocking effects that exhibit in the homogeneous regions of the images. Compressed images of ''Lena,'' ''Jet,'' and ''Peppers'' at 0.52 bpp are given in Fig. 5.

Since our method is a BTC-related hybrid method that uses classification skill (according to the local statistics of each block), we compared our results with some other BTC-related hybrid methods [VQ-IBTC (Ref. 9), BTC-CVQ (Ref. 7), HVQ (Ref. 11), adaptive compression coding (ACC) (Ref. 15), BTC-VQ-DCT (Ref. 8), VQ-BTC (Ref. 10), PDPCM-BTC (Ref. 16), and block pattern VQ (BPVQ) (Ref. 17)] and classified methods [BTC-CVQ, CVQ in DCT domain (Ref. 18), ACC, HVQ]. All data listed in Tables 2 to 4 for the reported methods are cited from the original papers (the only exception is the data for AMBTC, which were the simulation results quoted from Ref. 15). The reason that Table 2 is longer than Tables 3 and 4 is that the image ''Lena'' was used by more researchers in their reported papers than the images ''Jet'' and ''Peppers'' were. As for our method, the results about HABTC are provided from high bpp through low bpp, whereas the results about HABTC-VQ (the entries marked with an asterisk) are provided for low bpp only (because we had stated that the version with VQ is not worthy for high bpp). It is obvious that the proposed method can obtain higher PSNR by a bpp lower than the bpp needed by these BTC-related methods.

4 Conclusions

We have presented a hybrid compression technique, the HABTC method, to improve the bit rate of the BTC algorithm by incorporating some recently developed tech-

Fig. 5 Reconstructed images of the proposed HABTC method at 0.52 bpp: (a) ''Lena'' (32.28 in PSNR), (b) ''Jet'' (31.02 in PSNR), and (c) ''Peppers'' (32.66 in PSNR).

Table 2 Results generated by HABTC and other existing methods on the image ''Lena.''

bpp	PSNR for HABTC	PSNR for Existing Methods
2.11	38.09	
1.63		31.73 (AMBTC; Refs. 4 and 15)
1.5		34.85 (PDPCM-BTC; Ref. 16)
1.46		30.22 (BTC-CVQ; Ref. 7)
1.36		33.37 (ACC; Ref. 15)
1.3125		33.07 (BTC-VQ-DCT; Ref. 8)
1.25	36.24	33.01 (ACC; Ref. 15)
1.0		30.36 (PDPCM-BTC; Ref. 16)
1.0		30.59 (VQ-IBTC; Ref. 9)
0.99		33.98 (HQBPVQ; Ref. 17)
0.875		31.81 (BTC-VQ-DCT; Ref. 8)
0.83	34.44	
0.836		33.21 (VQ-BTC; Ref. 10)
0.813		32.57 (CVQ in DCT domain; Ref. 18)
0.8125		31.98 (BTC-VQ-DCT; Ref. 8)
0.76		28.95 (ACC; Ref. 15)
0.75		31.21 (BTC-VQ-DCT; Ref. 8)
0.75		32.23 (CVQ in DCT domain; Ref. 18)
0.75		29.30 (VQ-IBTC; Ref. 9)
0.715		32.81 (VQ-BTC; Ref. 10)
0.71	33.77	
0.6875		30.56 (BTC-VQ-DCT; Ref. 8)
0.625		31.26 (CVQ in DCT domain; Ref. 18)
0.62	33.18	
0.52		30.95 (BPVQ; Ref. 17)
0.48	32.01/32.32*	
0.398		29.52 (HVQ; Ref. 11)
0.37	30.87/31.35*	

*HABTC-VQ, i.e., the HABTC equipped with VQ.

Table 3 Results generated by HABTC and other existing methods on the image ''Jet.''

bpp	PSNR for HABTC	PSNR for Existing Methods
1.71	38.01	
1.63		30.48 (AMBTC; Refs. 4 and 15)
1.5		34.03 (PDPCM-BTC; Ref. 16)
1.33	37.30	
1.21		33.06 (ACC; Ref. 15)
1.14		34.87 (ACC; Ref. 15)
1.13	36.45	
1.0		28.96 (PDPCM-BTC; Ref. 16)
0.95		33.08 (HQBPVQ; Ref. 17)
0.872		33.51 (VQ-BTC; Ref. 10)
0.81		31.18 (ACC; Ref. 15)
0.76	33.85	
0.51		29.88 (BPVQ; Ref. 17)
0.50	30.73/31.47*	
0.41		29.06 (HVQ; Ref. 11)
0.39	29.10/29.96*	

*HABTC-VQ, i.e., the HABTC equipped with VQ.

Table 4 Results generated by HABTC and other existing methods on the image ''Peppers.''

bpp	PSNR for HABTC	PSNR for Existing Methods
2.22	38.15	
1.63		33.03 (AMBTC; Refs. 4 and 15)
1.5		34.19 (PDPCM-BTC; Ref. 16)
1.46	36.52	
1.30		34.88 (ACC; Ref. 15)
1.19	35.80	
1.17		34.60 (ACC; Ref. 15)
1.01	35.22	
1.0		29.47 (PDPCM-BTC; Ref. 16)
0.98		34.12 (HQBPVQ; Ref. 17)
0.81	34.41	
0.70		29.65 (ACC; Ref. 15)
0.56	32.91/33.22*	
0.50		29.94 (BPVQ; Ref. 17)
0.408		28.96 (HVQ; Ref. 11)
0.38	31.30/31.89*	

*HABTC-VQ, i.e., the HABTC equipped with VQ.

niques. Homogeneous blocks of the images are processed by the interpolation coding, predictive coding, or the uniform coding techniques to reduce the bit rate greatly. Inhomogeneous blocks are handled using four-level BTC whose thresholds are determined by the RWM bisection tool. Experimental results show that the compression ratios and PSNR values of the proposed method outperform those of many other BTC-related methods. (For the image ''Lena,'' the PSNR value is about 31 when the bit rate is 0.37 bpp.)

Acknowledgments

This work was supported by the National Science Council, Republic of China, under grant NSC85-2213-E009-111.

References

1. M. Rabbani and P. W. Jones, ''Transform coding,'' Chap. 10 in *Digital Image Compression Techniques*, pp. 102–128, SPIE Optical Engineering Press, Bellingham, WA (1991).
2. N. M. Nasrabadi and R. A. King, ''Image coding using vector quantization: a review,'' *IEEE Trans. Commun.* **36**(8), 957–971 (1988).
3. E. J. Delp and O. R. Mitchell, ''Image compression using block truncation coding,'' *IEEE Trans. Commun.* **27**(1), 1335–1342 (1979).
4. M. D. Lema and O. R. Mitchell, ''Absolute moment block truncation coding and application to color image,'' *IEEE Trans. Commun.* **32**(10), 1148–1157 (1984).
5. V. R. Udpikar and J. P. Raina, ''Modified algorithm for block truncation coding of monochrome images,'' *Electron. Lett.* **21**(20), 900–902 (1985).
6. V. R. Udpikar and J. P. Raina, ''BTC image coding using vector quantization,'' *IEEE Trans. Commun.* **35**(3), 352–356 (1987).
7. N. Efrati, H. Liciztin, and H. B. Mitchell, ''Classified block truncation coding-vector quantization: an edge sensitive image compression algorithm,'' *Signal Process. Image Commun.* **3**, 275–283 (1991).
8. Y. Wu and D. C. Coll, ''BTC-VQ-DCT hybrid coding of digital images,'' *IEEE Trans. Commun.* **39**(9), 1283–1287 (1991).
9. B. Zeng and Y. Neuvo, ''Interpolative BTC image coding with vector quantization,'' *IEEE Trans. Commun.* **41**(10), 1436–1438 (1993).
10. S. A. Mohamed and M. M. Fahmy, ''Image compression using VQ-BTC,'' *IEEE Trans. Commun.* **43**(7), 2177–2182 (1995).
11. K. A. Wen and C. Y. Lu, ''Hybrid vector quantization,'' *Opt. Eng.* **32**(7), 1496–1502 (1993).
12. P. A. Dondes and A. Rosenfeld, ''Pixel classification based on gray level and local business,'' *IEEE Trans. Pattern Anal. Mach. Intell.* **4**(1), 79–84 (1982).
13. C. Y. Yang and J. C. Lin, ''Use of radius weighted mean to cluster

two-class data,'' *Electron. Lett.* **30**(10), 757–759 (1994).
14. M. Kamel, C. T. Sun, and L. Guan, ''Image compression by variable block truncation coding with optimal threshold,'' *IEEE Trans. Image Process.* **39**(1), 208–212 (1991).
15. P. Nasiopoulos, R. K. Ward, and D. J. Morse, ''Adaptive compression coding,'' *IEEE Trans. Commun.* **39**(8), 1245–1254 (1991).
16. C. H. Chen and C. F. Chen, ''Progressive DPCM system with block truncation coding,'' *Electron. Lett.* **31**(21), 1821–1822 (1995).
17. S. A. Mohamed and M. M. Fahmy, ''Image compression using block pattern-vector quantization,'' *Signal Process.* **34**(1), 69–84 (1993).
18. D. S. Kim and S. U. Lee, ''Image vector quantizer based on a classification in the DCT domain,'' *IEEE Trans. Commun.* **39**(4), 549–556 (1991).

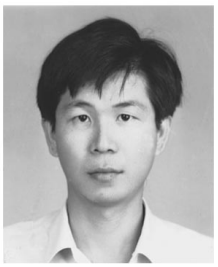

Ching-Yung Yang received his BS in electronic engineering in 1983 from National Taiwan Institute of Technology and his MS in electrical engineering in 1990 from National Cheng Kung University, Taiwan. From 1986 to 1988, he was a maintenance engineer at Central Taiwan Telecommunication Administration of the Ministry of Transportation and Communication, Taiwan. In 1992 he joined the Computer Vision Laboratory of the Department of Computer and Information Science at National Chiao Tung University, where he is currently a PhD candidate. His recent research interests include pattern recognition, image compression, and vector quantization. Mr. Yang is a member of the Chinese Image Processing and the Pattern Recognition Society.

Ja-Chen Lin received his BS in computer science in 1977 and his MS in applied mathematics in 1979, both from National Chiao Tung University, Taiwan. In 1988 he received his PhD in mathematics from Purdue University. From 1981 to 1982, he was an instructor at National Chiao Tung University. From 1984 to 1988, he was a graduate instructor at Purdue University. In August 1988 he joined the Department of Computer and Information Science at National Chiao Tung University, where he is currently a professor. His recent research interests include pattern recognition, image processing, and parallel computing. Dr. Lin is a member of the Phi-Tau-Phi Scholastic Honor Society, the Image Processing and Pattern Recognition Society, and the IEEE Computer Society.